Inorg. Chem. **2007**, *46*, 1297–1304

Heteronuclear Complexes of Macrocyclic Oxamide with Co-ligands: Syntheses, Crystal Structures, and Magnetic Properties

Li-Na Zhu,[†,||] Na Xu,[†] Wei Zhang,[‡,§] Dai-Zheng Liao,*[,†] Kazuyoshi Yoshimura,[‡] Ko Mibu,[§] Zong-Hui Jiang,[†] Shi-Ping Yan,[†] and Peng Cheng[†]

Department of Chemistry, Nankai University, Tianjin, 300071, China, Department of Chemistry, Graduate School of Science, Kyoto University, Kyoto, 606-8502, Japan, Research Center for Low Temperature and Materials Sciences, Kyoto University, Uji, Kyoto 611-0011, Japan, and Department of Chemistry, Tianjin University, Tianjin 300072, China

Received September 21, 2006

Four heteronuclear complexes $Mn(CuL)_2(SCN)_2$ (**1**), $\{[Mn(CuL)_2(\mu\text{-dca})_2]\cdot 2H_2O\}_n$ (**2**), $Zn(CuL)_2(SCN)_2$ (**3**), and $[Fe(CuL)(N_3)_2]_2$ (**4**) incorporating macrocyclic oxamide ligands have been synthesized and structurally characterized. L is the dianion of diethyl 5,6,7,8,15,16-hexahydro-6,7-dioxodibenzo[1,4,8,11]-tetraazacyclotetradecine-13,18-dicarboxylate, and dca is the dicyanamide. The structure of **1** or **3** consists of oxamido-bridged trinuclear $[M^{II}Cu^{II}_2]$ molecules (for **1**, M is the manganese(II) ion, and for **3**, M is the zinc(II) ion). Both of them consist of 1D supramolecuar chains via π–π interactions. The structure of **2** also has the oxamido-bridged trinuclear $[Mn^{II}Cu^{II}_2]$ structure units and consists of 2D layers formed by the linkage of copper(II) and manganese(II) atoms via the oxamido and $\mu_{1,5}$-dca bridges. Complex **4** consists of oxamido-bridged tetranuclear $[Fe^{II}_2Cu^{II}_2]$ molecules and arranges in 1D chains. Different co-ligands may result in different structures in this macrocyclic oxamide system. The variable-temperature magnetic susceptibility measurements (2–300 K) of **1** and **2** both show the pronounced antiferromagnetic interactions between the copper(II) and manganese(II) ions.

Introduction

Polynuclear complexes are of considerable interest for the design of new magnetic materials and the investigation of the structure and the role of the polymetallic active sites in biological systems.[1] Among polynuclear complexes, heterospin complexes have received particular attention. The magnetic interaction between two nonequivalent paramagnetic centers may lead to a situation that cannot be encountered with species containing only one kind of center, but heterospin complexes can provide various and unexpected structural topologies.[2] From the magnetic viewpoint, the magnetic interaction between nearest nonequivalent neighbor spin carriers may be ferromagnetic; it may also be antiferromagnetic with a noncompensation of the local spins. In the latter case, the most favorable situation is that the difference between the nonequivalent local spins is as large as possible. The synthesis and magnetic investigation of manganese(II)−copper(II) complexes with $S_{Mn} = 5/2$ and $S_{Cu} = 1/2$ local spins therefore is one active facet of the molecular magnetism. The first molecular-based heterobimetallic magnets were the oxamato- and oxamido-bridged manganese(II)−copper(II) species.[3]

N,*N*′-bis(coordinating group-substituted) oxamides are well-known good building blocks of the polynuclear com-

* To whom correspondence should be addressed. Fax: +86-22-23502779. E-mail: coord@nankai.edu.cn.
† Department of Chemistry, Nankai University.
‡ Department of Chemistry, Graduate School of Science, Kyoto University.
§ Research Center for Low Temperature and Materials Sciences, Kyoto University.
|| Department of Chemistry, Tianjin University.

(1) (a) Kahn, O. *Molecular Magnetism*; VCH: New York, 1993. (b) Gatteschi, D.; Kahn, O.; Miller, J. S.; Palacio, F. *Molecular Magnetic Materials*; NATO ASI Series; Kluwer: Dordrecht, The Netherlands, 1991. (c) Coronado, E.; Delhaès, P.; Gatteschi, D.; Miller, J. S. *Molecular Magnetism: From Molecular Assemblies to the Devices*; Kluwer: Dordrecht, The Netherlands, 1996. (d) Gatteschi, D.; Caneschi, A.; Sessoli, R.; Cornia, A. *Chem. Soc. Rev.* **1996**, 101.

(2) (a) Kahn, O. *Adv. Inorg. Chem.* **1996**, *43*, 179. (b) Kahn, O.; Galy, J.; Journaux, Y.; Jaud, J.; Morgestern-Badarau, I. *J. Am. Chem. Soc.* **1982**, *104*, 2165. (c) Baron, V.; Gillon, B.; Plantevin, O.; Cousson, A.; Mathonière, C.; Kahn, O.; Grand, A.; Öhrström, L.; Delley, B. *J. Am. Chem. Soc.* **1996**, *118*, 11822. (d) Sato, O.; Iyoda, T.; Fujishima, A.; Hashimoto, K. *Science* **1996**, *271*, 49.

(3) (a) Kahn, O.; Pei, Y.; Verdaguer, M.; Renard, J. P.; Sletten, J. *J. Am. Chem. Soc.* **1988**, *110* (3), 782. (b) Nakatani, K.; Carriat, J. Y.; Journaux, Y.; Kahn, O.; Lloret, F.; Renard, J. P.; Pei, Y.; Sletten, J.; Verdaguer, M. *J. Am. Chem. Soc.* **1989**, *111*, 5739.

10.1021/ic061792m CCC: $37.00
Published on Web 01/23/2007

Scheme 1. Some Mononuclear Cu(II) Complexes of the Macrocyclic Oxamide Used as the Complex Ligands

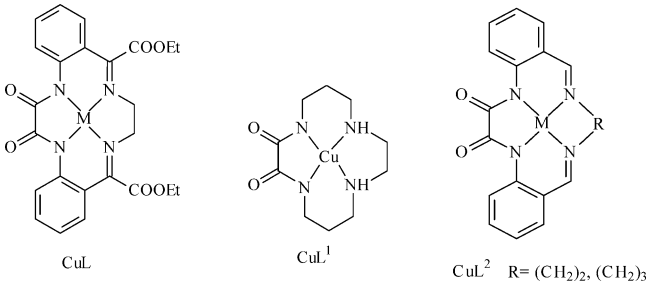

plexes, which can give rise to a rich variety of complexes and extended structures via the cis or trans conformation.[3−8] The macrocyclic oxamides, in which the exo−cis conformation of the oxygen donors is enforced, allow us to synthesize heterobimetallic systems and model magnetic systems in a more controlled fashion via the stepwise complexation of the macrocyclic and exo donors (Scheme 1).[9] Compared with the polymetallic systems of noncyclic oxamides, those containing macrocyclic oxamides are limited, although complexes of macrocyclic ligands have been of great interest to supramolecular and coordination chemists for their special structures, properties, and functionalities.[10] Christodoulou and his colleagues reported two bimetallic complexes by using a mononuclear diamagnetic nickel(II) complex of the macrocyclic oxamide as a complex ligand.[11] Robertson and his colleagues first reported a mononuclear paramagnetic copper(II) complex of the macrocyclic oxamide ([CuL^1], Scheme 1) and obtained a trinuclear copper(II) complex derived from it.[9] After this, a series of bi-,[12−14] tetra-,[15−16] penta-,[17−18] hexa-,[18] and nonanuclear[19] 1-[20] and 2D[21] complexes producedusing the mononuclear copper(II) precursors[22] of macrocyclic oxamides (Scheme 1) have been reported. As far as the oxamido-bridged macrocyclic complexes are concerned, only few examples based on the [M^{II}-Cu^{II}(μ-oxamidato)][13,20] or [M^{II}Cu$^{II}_3$(μ-oxamidato)$_3$][15−16] unit have been structurally characterized.

With these facts in mind and in continuation of our earlier work, we report the syntheses, crystal structures, and magnetic properties of four new bimetallic complexes Mn(CuL)$_2$(SCN)$_2$ (**1**), {[Mn(CuL)$_2$(μ-dca)$_2$]·2H$_2$O}$_n$ (**2**), Zn(CuL)$_2$(SCN)$_2$ (**3**), and [Fe(CuL)(N$_3$)$_2$]$_2$ (**4**) incorporating a macrocyclic oxamide ligand. L is the dianion of diethyl 5,6,7,8,15,16-hexahydro-6,7-dioxodibenzo[1,4,8,11]-tetraazacyclotetradecine-13,18-dicarboxylate, and dca is the dicyanamide. Complexes **1** and **3** consist of 1D supramolecular chains via $\pi-\pi$ interactions; **2** is composed of 2D layers, and **4** made of 1D chains. The magnetic properties of **1** and **2** are also reported.

Experimental Section

Materials. All chemicals were of reagent grade and were used as received. The mononuclear precursor [CuL] was prepared as described elsewhere.[22]

Caution: Perchlorate salts are potentially explosive and should therefore be handled with appropriate care.

Synthesis of 1. Solid samples of Mn(ClO$_4$)$_2$·6H$_2$O (0.1 mmol) and NaSCN (0.2 mmol) were added to a suspension of [CuL] (0.2 mmol) in EtOH (40 mL). The mixture was stirred under reflux for 10 h and then left to cool. The resulting small quantity of precipitates was filtered off. Brown crystals were obtained by slow evaporation of the filtrate at room temperature. Yield: 40%. IR (KBr, cm^{-1}): 3480br, 2150vs, 1735s, 1638vs, 1615s, 1590s, 1570s, 1465 m, 1350s, 1283w, 1224s, 1060w, 1043m, 940m, 788w, 760m,

(4) (a) Ojima, H.; Nonoyama, K. *Coord. Chem. Rev.* **1988**, *92*, 85. (b) Ruiz, R.; Faus, J.; Lloret, F.; Julve, M.; Journaux, Y. *Coord. Chem. Rev.* **1999**, *193*, 1069.
(5) Lloret, F.; Journaux, Y.; Julve, M. *Inorg. Chem.* **1990**, *29*, 3967.
(6) (a) Okawa, H.; Kawahara, Y.; Masahiro, M.; Kida, S. *Bull. Chem. Soc. Jpn.* **1980**, *53*, 549. (b) Banci, L.; Bencini, A.; Benelli, C.; Getteschi, D. *Inorg. Chem.* **1981**, *20*, 1399. (c) Journaux, Y.; Sletten, J.; Kahn, O. *Inorg. Chem.* **1985**, *24*, 4063. (d) Journaus, Y.; Sletten, J.; Kahn, O. *Inorg. Chem.* **1986**, *25*, 439. (e) Lloret, F.; Julve, M.; Faus, J.; Ruiz, R.; Castro, I.; Mollar, M.; Philoche-Levisalles, M. *Inorg. Chem.* **1992**, *31*, 784. (f) Escuer, A.; Vicente, R.; Ribas, J.; Costa, R.; Solans, X. *Inorg. Chem.* **1992**, *31*, 2627. (g) Lloret, F.; Julve, M.; Ruiz, R.; Journaux, Y.; Nakatani, K.; Kahn, O.; Sletten, J. *Inorg. Chem.* **1993**, *32*, 27. (h) Mathoniére, C.; Kahn, O.; Daran, J. C.; Hilbig, H.; Köhler, F. H. *Inorg. Chem.* **1993**, *32*, 4057.
(7) (a) Zhang, Z. Y.; Liao, D. Z.; Jiang, Z. H.; Hao, S. Q.; Yao, X. K.; Wang, H. G.; Wang, G. L. *Inorg. Chim. Acta* **1990**, *173*, 201. (b) Real, J. A.; Ruiz, R.; Faus, J.; Julve, M.; Journaux, Y.; Phioche-Levisalles, M.; Bois, C. *J. Chem. Soc., Dalton Trans.* **1994**, 3769. (c) Sanz, J. L.; Ruiz, R.; Gleizes, A.; Lloret, F.; Faus, J.; Julve, M.; Borrás-Almenar, J. J.; Journaux, Y. *Inorg. Chem.* **1996**, *35*, 7384. (d) Larionova, J.; Chavan, S. A.; Yakhmi, J. V.; Frøystein, A. G.; Sletten, J.; Sourisseau, C.; Kahn, O. *Inorg. Chem.* **1997**, *36*, 6374. (e) Chen, Z. N.; Zhang, H. X.; Yu, K. B.; Kang, B. S.; Cai, H.; Su, C. Y.; Wang, T. W.; Lu, Z. L. *Inorg. Chem.* **1998**, *37*, 4475. (f) Ribas, J.; Diaz, C.; Costa, R.; Tercero, J.; Solans, X.; Font-Bardía, M.; Stoeckli-Evans, H. *Inorg. Chem.* **1998**, *37*, 223.
(8) (a) Dominguez-Vera, J. M.; Moreno, J. M.; Galvez, N.; Suarez-Varela, J.; Colacio, E.; Kivekas, R.; Klinga, M. *Inorg. Chim. Acta* **1998**, *281*, 95. (b) Diaz, C.; Ribas, J.; Costa, R.; Tercero, J.; El Fallah, M. S.; Solans, X.; Font-Bardía, M. *Eur. J. Inorg. Chem.* **2000**, 675. (c) Castro, I.; Calatayud, M. L.; Sletten, J.; Julve, M.; Llort, F. *C. R. Acad. Sci. Ser. IIc: Chim.* **2001**, 235. (d) Fukita, N.; Ohba, M.; Shiga, T.; Ōkawa, H.; Ajiro, Y. *J. Chem. Soc., Dalton Trans.* **2001**, 64. (e) Zang, S. Q.; Tao, R. J.; Wang, Q. L.; Hu, N. H.; Cheng, Y. X.; Niu, J. Y.; Liao, D. Z. *Inorg. Chem.* **2003**, *42*, 761.
(9) Cronin, L.; Mount, A. R.; Parsons, S.; Robertson, N. *J. Chem. Soc., Dalton Trans.* **1999**, 1925.
(10) (a) Melson, G. A. *Coordination Chemistry of Macrocyclic Compounds*; Plenum: New York, 1979. (b) Vigato, P. A.; Tamburini, S.; Fenton, D. E. *Coord. Chem. Rev.* **1990**, *106*, 25. (c) Chen, C. T.; Suslick, K. S. *Coord. Chem. Rev.* **1993**, *128*, 293.
(11) Christodoulou, D.; Kanatzidis, M. G.; Coucouvanis, D. *Inorg. Chem.* **1990**, *29*, 191.
(12) Gao, E. Q.; Tang, J. K.; Liao, D. Z.; Jiang, Z. H.; Yan, S. P.; Wang, G. L. *Helv. Chim. Acta* **2001**, *84*, 908.
(13) (a) Tang, J. K.; Wang, L. Y.; Zhang, L.; Gao, E. Q.; Liao, D. Z.; Jiang, Z. H.; Yan, S. P.; Cheng, P. *J. Chem. Soc., Dalton Trans.* **2002**, 1607. (b) Tang, J. K.; Si, S. F.; Wang, L. Y.; Liao, D. Z.; Jiang, Z. H.; Yan, S. P.; Cheng, P.; Liu, X. *Inorg. Chim. Acta* **2003**, *343*, 288.
(14) (a) Tang, J. K.; Si, S. F.; Wang, L. Y.; Liao, D. Z.; Jiang, Z. H.; Yan, S. P.; Cheng, P.; Liu, X. *Inorg. Chem. Comm.* **2002**, *5*, 1012. (b) Tang, J. K.; Si, S. F.; Gao, E. Q.; Liao, D. Z.; Jiang, Z. H.; Yan, S. P. *Inorg. Chim. Acta* **2002**, *332*, 146.
(15) Tang, J. K.; Wang, Q. L.; Gao, E. Q.; Chen, J. T.; Liao, D. Z.; Jiang, Z. H.; Yan, S. P.; Cheng, P. *Helv. Chim. Acta* **2002**, *85*, 175.
(16) Liu, Z. L.; Zhang, D. Q.; Luo, J. L.; Jiang, Z. H.; Liao, D. Z.; Zhu, D. B. *J. Coord. Chem.* **2004**, *57*, 647.
(17) Sun, Y. Q.; Yang, G. M., Liao, D. Z.; Jiang, Z. H.; Yan, S. P. *Inorg. Chem. Commun.* **2003**, *6*, 799.
(18) Sun, Y. Q.; Liang, M; Dong, W; Yang, G. M., Liao, D. Z.; Jiang, Z. H.; Yan, S. P.; Cheng, P. *Eur. J. Inorg. Chem.* **2004**, *7*, 1514.
(19) Tang, J. K.; Li, Y. Z.; Wang, Q. L.; Gao, E. Q.; Liao, D. Z.; Jiang, Z. H.; Yan, S. P.; Cheng, P.; Wang, L. F.; Wang, G. L. *Inorg. Chem.* **2002**, *41*, 2188.
(20) Wang, S. B.; Yang, G. M.; Liao, D. Z.; Li, L. C. *Inorg. Chem.* **2004**, *43*, 852.
(21) Sun, Y. Q.; Tian, J. L.; Dong, W; Yang, G. M., Liao, D. Z.; Jiang, Z. H.; Yan, S. P. *Inorg. Chem. Commun.* **2004**, *7*, 137.
(22) Gao, E. Q.; Bu, W. M.; Yang, G. M.; Liao, D. Z.; Jiang, Z. H.; Yan, S. P.; Wang, G. L. *J. Chem. Soc., Dalton Trans.* **2000**, 1431.

Table 1. Crystal Data and Structure Refinement for Complexes **1**, **2**, **3**, and **4**

	1	**2**	**3**	**4**
empirical formula	$C_{50}H_{44}Cu_2MnN_{10}O_{12}S_2$	$C_{52}H_{48}Cu_2MnN_{14}O_{14}$	$C_{50}H_{44}Cu_2N_{10}O_{12}S_2Zn$	$C_{24}H_{22}CuFeN_{10}O_6$
fw	1223.09	1275.06	1233.52	665.91
cryst syst	monoclinic	monoclinic	monoclinic	triclinic
space group	*C2/c*	*C2/c*	*C2/c*	$P\bar{1}$
a (Å)	21.229(6)	39.131(9)	21.208(7)	10.763(4)
b (Å)	14.169(4)	13.082(3)	14.214(5)	11.936(4)
c (Å)	17.183(5)	28.121(7)	17.062(6)	12.510(7)
α (deg)	90	90	90	101.378(6)
β (deg)	95.085(5)	114.530(4)	95.39	106.967(6)
γ (deg)	90	90	90	116.291(4)
V (Å^3)	5148(2)	13096(6)	5121(3)	1274.4(10)
Z	4	8	4	2
ρ_{calcd} (g · cm^{-3})	1.578	1.293	1.600	1.735
abs coeff (mm^{-1})	1.215	1.900	1.443	1.467
cryst size (mm^3)	0.24 × 0.20 × 0.14	0.20 × 0.16 × 0.14	0.46 × 0.14 × 0.08	0.44 × 0.12 × 0.08
θ range (deg)	1.73−25.01	− 25.00	1.73−25.03	1.84−25.03
independent reflns	4547 [R_{int} = 0.0650]	11 552 [R_{int} = 0.0800]	4523 [R_{int} = 0.0296]	4420 [R_{int} = 0.0183]
Final R indices [$I > 2\sigma(I)$]	R1 = 0.0466, wR2 = 0.0969	R1 = 0.0792, wR2 = 0.2258	R1 = 0.0310, wR2 = 0.0754	R1 = 0.0407, wR2 = 0.1137
R indices (all data)	R1 = 0.0989, wR2 = 0.1265	R1 = 0.1571, wR2 = 0.2819	R1 = 0.0471, wR2 = 0.0814	R1 = 0.0583, wR2 = 0.1210

680m. Anal. Calcd for $C_{50}H_{44}Cu_2MnN_{10}O_{12}S_2$: C, 49.10; H, 3.63; N, 11.45. Found: C, 49.23; H, 3.68; N, 11.37%.

Synthesis of 2. The complex was obtained following the procedure described above for **1** except that $NaN(CN)_2$ was substituted for NaSCN. The crystals were black. Yield: 63%. IR (KBr, cm^{-1}): 3500br, 2349w, 2285w, 2230vs, 1738s, 1636s, 1610s, 1590s, 1565s, 1490m, 1459m, 1346s, 1273w, 1214s, 1182w, 1150w, 1079w, 1049m, 1023m, 937m, 782w, 761m, 675w. Anal. Calcd for $C_{52}H_{48}Cu_2MnN_{14}O_{14}$: C, 48.98; H, 3.79; N, 15.38. Found: C, 49.07; H, 3.74; N, 15.37%.

Synthesis of 3. The complex was obtained following the procedure described above for **1** except that $Zn(ClO_4)_2 \cdot 6H_2O$ was substituted for $Mn(ClO_4)_2 \cdot 6H_2O$. The crystals were brown. Yield: 43%. IR (KBr, cm^{-1}): 3400br, 2120s, 1738s, 1636vs, 1612s, 1590s, 1568s, 1469m, 1346s, 1216s, 1042m, 937m. Anal. Calcd for $C_{50}H_{44}Cu_2N_{10}O_{12}S_2Zn$: C, 48.68; H, 3.60; N, 11.35. Found: C, 48.56; H, 3.55; N, 11.40%.

Synthesis of 4. The complex was obtained following the procedure described above for **1** except that $Fe(ClO_4)_2 \cdot 6H_2O$ and NaN_3 were substituted for $Mn(ClO_4)_2 \cdot 6H_2O$ and NaSCN, respectively. The crystals were deep green. Yield: 55%. IR (KBr, cm^{-1}): 3400br, 2070s, 1736s, 1638vs, 1610s, 1592s, 1575s, 1465m, 1347s, 1224s, 1045m, 940m. Anal. Calcd for $C_{24}H_{22}CuFeN_{10}O_6$: C, 43.29; H, 3.33; N, 21.03. Found: C, 43.15; H, 3.36; N, 21.11%.

Physical Measurements. Elemental analyses (C, H, N) were performed on a Perkin−Elmer 240 analyzer. The FT-IR spectra were measured with a Bruker Tensor 27 Spectrometer on KBr disks in the region of 4000−400 cm^{-1}. Variable-temperature magnetic susceptibilities were measured on a Quantum Design MPMS 5S SQUID magnetometer in the temperature range of 2−300 K. Diamagnetic corrections were made with Pascal's constants for all the constituent atoms.[23]

Crystal Structure Determination and Refinement. Determination of the unit cell and data collection were performed at 293 K on a BRUKER SMART 1000 area detector using graphite-monochromated Mo Kα radiation (λ = 0.71073 Å). The structures were solved by direct methods using SHELXS-97 and refined by least-squares procedures on F_o^2 with SHELXL-97 by minimizing the function $\sum w(F_o^2 - F_c^2)$,[2] where F_o and F_c are the observed and calculated structure factors, respectively.[24] The hydrogen atoms were located geometrically and refined isotropically. Crystal data collection and refinement parameters are given in Table 1.

Results and Discussion

So far, only two binuclear complexes derived from [CuL] and its derivative have been crystallographically characterized because of synthetic difficulties.[12] From the comparison of a variety of polynuclear complexes from [CuL^1][9,13−15,19] and [CuL^2],[16−18,20−21] it seems that the huge bulk of the complex precursor [CuL] hinders the ability to obtain the crystal and to determine the structural extent of the polynuclear complex. However, by suitable choice of the co-ligand, we can improve the crystallization of the products and also can obtain the extended structures. As far as the M(II)−copper-(II) heteronuclear systems are concerned, we have tried many times to obtain a crystal suitable for the X-ray diffraction by reacting [CuL] directly with M(II) (M(II) is transition metal ion) salts in the solution. All attempts were in vain. The thiocyanate, dicyanamide, and azide are well-known building blocks as the teminal or bridging ligands and easily lead to the crystals with metal ions and other ligands. Thus we chose the thiocyanate, dicyanamide, and azide as the co-ligands and obtained two 1D supermolecular chains, a 2D layer, and a 1D chain heterometallic complexes by the self-assembly of the building block [CuL] and M(II) (M = Mn, Zn, Fe) with co-ligands.

IR Spectra. The IR spectra of the four complexes are similar and clearly show the existence of the thiocyanate, dicyanamide, or azide and macrocyclic oxamide moieties in the molecules. The band at 2150 cm^{-1} in the spectra of **1** or **3** and the split bands at 2349, 2285, and 2230 cm^{-1} in **2** can be attributed to the ν(C≡N) stretching absorption, indicating the existence of the thiocyanate and dicyanamide moieties,

(23) Selwood, P. W. *Magnetochemistry*; Interscience: New York, 1956; p 78.

(24) Sheldrick, G. M. *SHELXS-97* and *SHELXL-97, Software for Crystal Structure Analysis*; Siemens Analytical X-ray Instruments Inc.: Madison, WI, 1997.

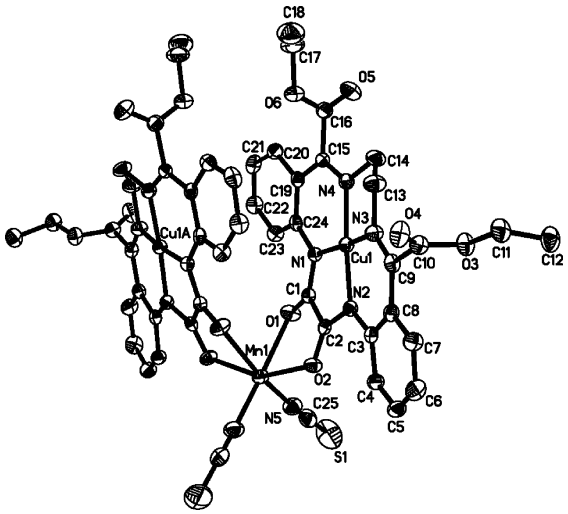

Figure 1. ORTEP view and atom labeling of the trinuclear molecule for **1**. Thermal ellipsoids at the 30% level are shown.

Table 2. Selected Bond Lengths (Å) and Angles (deg) for **1**[a]

Cu(1)−N(2)	1.929(4)	Mn(1)−N(5)	2.111(5)
Cu(1)−N(4)	1.932(4)	Mn(1)−O(2)	2.189(3)
Cu(1)−N(1)	1.936(3)	Mn(1)−O(1)	2.288(3)
Cu(1)−N(3)	1.947(4)		
N(2)−Cu(1)−N(4)	176.17(15)	N(5)#1−Mn(1)−O(2)	94.66(14)
N(2)−Cu(1)−N(1)	88.12(14)	O(2)−Mn(1)−O(2)#1	153.90(17)
N(4)−Cu(1)−N(1)	93.97(15)	N(5)−Mn(1)−O(1)#1	161.01(14)
N(2)−Cu(1)−N(3)	93.13(15)	O(2)−Mn(1)−O(1)#1	87.88(12)
N(4)−Cu(1)−N(3)	85.12(15)	N(5)−Mn(1)−O(1)	93.06(15)
N(1)−Cu(1)−N(3)	174.09(16)	O(2)−Mn(1)−O(1)	71.16(11)
N(5)−Mn(1)−N(5)#1	102.4(3)	O(1)#1−Mn(1)−O(1)	74.33(18)
N(5)−Mn(1)−O(2)	101.64(14)		

[a] Symmetry transformations used to generate equivalent atoms: #1 $-x+1, y, -z+1/2$.

respectively.[25−26] In **4**, the band at 2070 cm^{-1} is caused by the existence of azide. The bands at ~1735 and 1610 cm^{-1}, which show no significant shift relative to corresponding bonds of the mononuclear precursor [CuL], are attributed to ν(C═O) (ester) and ν(C═N), respectively.[22] The strong ν-(C═O) (oxamido) band at ~1650 cm^{-1} in the spectrum of the mononuclear precursor is replaced by a strong band at 1638 cm^{-1} in **1**, 1636 cm^{-1} in **2**, and 1637 cm^{-1} in **3** and **4**.[22] The bathochromic shift is consistent with the change in the C═O bond lengths on coordination, as confirmed by the X-ray crystallographic studies.

Description of the Structure of 1. The structure of **1** consists of trinuclear $Mn(CuL)_2(SCN)_2$ molecules in which the central manganese(II) ion is located on a two-fold axis and linked to two [CuL] complex ligands and two thiocyanate ligands in a *cis* configuration. An ORTEP drawing of **1** with the atom numbering scheme is given in Figure 1. Selected bond lengths and angles are given in Table 2.

The copper(II) atom resides in a slightly distorted square-planar environment with two amidate nitrogen atoms and two imino nitrogen atoms from the macrocyclic oxamide ligand as donors. The deviations of the four donor atoms (N1−N4) from their mean plane are 0.0760, −0.0763, 0.0782, and −0.0779 Å, respectively. The distance between the copper atom in the plane is −0.0213 Å. The manganese-(II) atom has a cis octahedral geometry with four oxygen atoms from two oxamido bridges and two nitrogen atoms from two thiocyanate ligands. The central manganese(II) atom is linked to each external copper(II) atom via the exo−cis oxygen donors of the macrocyclic oxamide ligand. The three metal atoms form a U-type arrangement through the oxamido bridges with a Cu···Mn separation of 5.392 Å and a Cu···Cu separation of 6.817 Å (Figure 1).

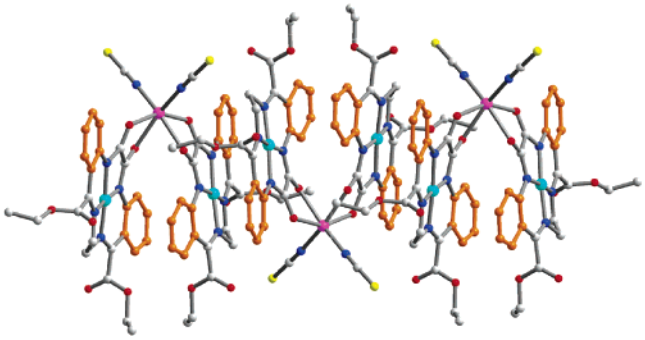

Figure 2. 1D supramolecuar chain for **1** constructed by the head-to-tail arrangement of the adjacent trinuclear molecules via $\pi-\pi$ interactions. Color scheme: cyan spheres, Cu(II); pink spheres, Mn(II); red spheres, O; blue spheres, N; yellow spheres, S; gray spheres, C not belonging to the phenyl ring; gold, C belonging to the phenyl ring.

The striking feature of **1** is the interesting arrangement of the adjacent trinuclear molecules. As depicted in Figure 2, a linear chain is constructed by the "head-to-tail" arrangement of the adjacent trinuclear molecules. There are $\pi-\pi$ interactions in the overlapped [CuL] fragments from the adjacent trinuclear molecules. The C3−C8 ring from one [CuL] fragment and the C19−C24 ring from its adjacent [CuL] fragment are almost parallel with a dihedral angle of 170.2°, and the ring centroid−centroid distance is 3.741 Å. For the adjacent trinuclear molecules, the Cu···Cu and Cu···Mn separations are 3.943 and 5.720 Å, respectively. The $\pi-\pi$ interactions organize the trinuclear molecules into a compact 1D supramolecular chain and also enhance the stability of **1**.

Description of the Structure of 2. The structure unit of **2** is shown in Figure 3 (free water molecules are omitted for clarity). Selected bond lengths and angles are given in Table 3.

Each structure unit consists of a heterotrinuclear $Cu^{II}Mn^{II}$-Cu^{II} moiety and two free water molecules. The central manganese(II) atom is linked to two asymmetric external copper(II) atoms via the exo−cis oxygen donors of the macrocyclic oxamide ligand and two dca ligands in a cis configuration. The manganese(II) ion has a distorted octahedral geometry with four oxygen atoms from two oxamido bridges and two nitrogen atoms from two dca ligands. The Cu(II) atom resides in a slightly distorted square pyramidal environment. Four nitrogen donors from the macrocyclic ligand coordinate to the Cu(II) atom as the square base of the pyramid with the nearly equivalent Cu−N bond lengths. One nitrogen donor from the dca ligand of the adjacent

(25) Groeneveld, L. R.; Vos, G.; Verschoor, G. C.; Reedijk, J. *J. Chem. Soc., Chem. Commun.* **1982**, 620.
(26) Manson, J. L; Kmety, C. R.; Epstein, A. J.; Miller, J. S. *Inorg. Chem.* **1999**, *38*, 2552.

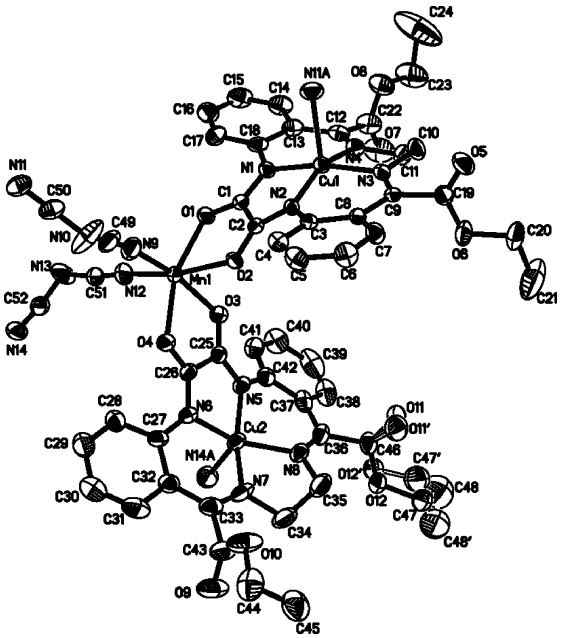

Figure 3. ORTEP view and atom labeling of the asymmetric unit for **2**. Thermal ellipsoids at the 30% level are shown, and free water molecules are omitted for clarity.

Table 3. Selected Bond Lengths (Å) and Angles (deg) for **2**[a]

Cu(1)−N(2)	1.950(5)	Cu(2)−N(8)	1.986(8)
Cu(1)−N(1)	1.954(6)	Cu(2)−N(14)#2	2.171(8)
Cu(1)−N(3)	1.964(6)	Mn(1)−O(1)	2.157(5)
Cu(1)−N(4)	1.967(6)	Mn(1)−N(9)	2.163(9)
Cu(1)−N(11)#1	2.287(8)	Mn(1)−O(4)	2.165(5)
Cu(2)−N(5)	1.923(7)	Mn(1)−N(12)	2.179(8)
Cu(2)−N(6)	1.952(6)	Mn(1)−O(3)	2.219(6)
Cu(2)−N(7)	1.971(8)	Mn(1)−O(2)	2.251(5)
N(2)−Cu(1)−N(1)	85.2(2)	N(7)−Cu(2)−N(14)#2	97.1(3)
N(2)−Cu(1)−N(3)	92.9(2)	N(8)−Cu(2)−N(14)#2	99.2(3)
N(1)−Cu(1)−N(3)	167.7(3)	O(1)−Mn(1)−N(9)	102.6(3)
N(2)−Cu(1)−N(4)	156.4(2)	O(1)−Mn(1)−O(4)	160.6(2)
N(1)−Cu(1)−N(4)	91.5(3)	N(9)−Mn(1)−O(4)	91.3(3)
N(3)−Cu(1)−N(4)	85.3(3)	O(1)−Mn(1)−N(12)	94.0(3)
N(2)−Cu(1)−N(11)#1	110.7(3)	N(9)−Mn(1)−N(12)	95.4(3)
N(1)−Cu(1)−N(11)#1	97.1(3)	O(4)−Mn(1)−N(12)	98.1(3)
N(3)−Cu(1)−N(11)#1	94.9(3)	O(1)−Mn(1)−O(3)	90.4(2)
N(4)−Cu(1)−N(11)#1	92.9(3)	N(9)−Mn(1)−O(3)	164.4(3)
N(5)−Cu(2)−N(6)	84.9(3)	O(4)−Mn(1)−O(3)	74.1(2)
N(5)−Cu(2)−N(7)	161.9(3)	N(12)−Mn(1)−O(3)	92.2(3)
N(6)−Cu(2)−N(7)	91.6(3)	O(1)−Mn(1)−O(2)	74.12(19)
N(5)−Cu(2)−N(8)	90.0(3)	N(9)−Mn(1)−O(2)	86.4(3)
N(6)−Cu(2)−N(8)	152.7(3)	O(4)−Mn(1)−O(2)	93.6(2)
N(7)−Cu(2)−N(8)	84.9(4)	N(12)−Mn(1)−O(2)	168.1(3)
N(5)−Cu(2)−N(14)#2	100.9(3)	O(3)−Mn(1)−O(2)	88.9(2)
N(6)−Cu(2)−N(14)#2	108.1(3)		

[a] Symmetry transformations used to generate equivalent atoms: #1 $-x + 3/2, y + 1/2, -z + 3/2$; #2 $-x + 1, y, -z + 3/2$.

trinuclear unit coordinates to the Cu(1) atom as the apex of the pyramid with the bond being a little longer.

As depicted in Figure 4 (only metal atoms and bridge atoms are left, other atoms are omitted for clarity), one asymmetric trinuclear unit connects to three adjacent equivalent units via the $\mu_{1,5}$-dca bridges: the $[Cu1Mn1Cu2]_A$ unit connects to the $[Cu1Mn1Cu2]_C$ unit through the Mn1A−dca−Cu2C and Mn1C−dca−Cu2A linkages, the $[Cu1Mn1Cu2]_A$ unit connects to the $[Cu1Mn1Cu2]_B$ unit through the Mn1B−dca−Cu1A linkage, and the $[Cu1Mn1Cu2]_A$ unit connects to the $[Cu1Mn1Cu2]_I$ unit through the Mn1A−dca−Cu1I

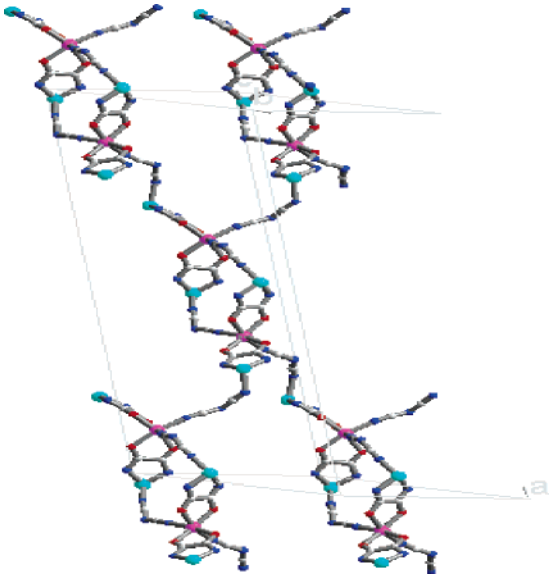

Figure 4. Schematic representation of one asymmetric oxamide-bridged trinuclear unit generating to a 2D layer of **2** via $\mu_{1,5}$-dca bridges. Only metal atoms and bridge atoms are left; the other atoms are omitted for clarity. Color scheme: cyan spheres, Cu(II); pink spheres, Mn(II); red spheres, O; blue spheres, N; gray spheres, C.

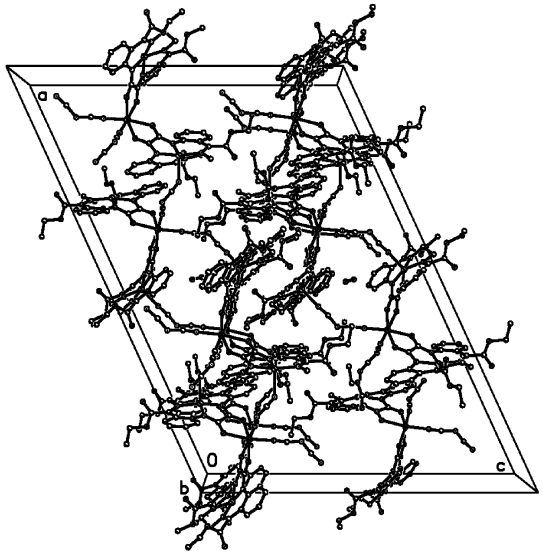

Figure 5. Molecule packing along the *b* axis for **2**.

linkage. In short, each triunclear unit is connected to three adjacent triunclear units through two kinds of the "interunit" Cu···Mn linkages, that is, Mn1−dca−Cu1 and Mn1−dca−Cu2 with a Cu···Mn separation of 7.906 and 8.252 Å, respectively. Then, the heterometallic atoms are linked each other though the oxamido and $\mu_{1,5}$-dca bridges, forming an extended 2D layer of **2**. The molecule packing along the *b* axis is shown in Figure 5. The parallel staggered layers stack and form a compact structure. Free water molecules reside in the vacancies of the molecular framework, and no hydrogen bond interaction exists.

Description of the Structure of 3. The structure of **3** is similar to **1**, except that Mn^{2+} was substituted with Zn^{2+}. Selected bond lengths and angles are given in Table 4.

Description of the Structure of 4. The structure unit of **4** is shown in Figure 6. Selected bond lengths and angles

Table 4. Selected Bond Lengths (Å) and Angles (deg) for **3**[a]

Zn(1)−N(5)#1	2.003(3)	Zn(1)−O(6)#1	2.2572(19)
Zn(1)−N(5)	2.003(3)	Cu(1)−N(2)	1.931(2)
Zn(1)−O(5)#1	2.1067(18)	Cu(1)−N(1)	1.938(2)
Zn(1)−O(5)	2.1067(18)	Cu(1)−N(3)	1.940(2)
Zn(1)−O(6)	2.2572(19)	Cu(1)−N(4)	1.944(2)
N(5)#1−Zn(1)−N(5)	103.02(15)	N(5)−Zn(1)−O(6)#1	162.10(9)
N(5)#1−Zn(1)−O(5)#1	101.59(9)	O(5)#1−Zn(1)−O(6)#1	73.20(7)
N(5)−Zn(1)−O(5)#1	94.41(9)	O(5)−Zn(1)−O(6)#1	86.17(7)
N(5)#1−Zn(1)−O(5)	94.41(9)	O(6)−Zn(1)−O(6)#1	74.35(10)
N(5)−Zn(1)−O(5)	101.59(9)	N(2)−Cu(1)−N(1)	87.95(8)
O(5)#1−Zn(1)−O(5)	154.20(10)	N(2)−Cu(1)−N(3)	94.01(9)
N(5)#1−Zn(1)−O(6)	162.10(9)	N(1)−Cu(1)−N(3)	176.74(9)
N(5)−Zn(1)−O(6)	92.30(9)	N(2)−Cu(1)−N(4)	173.71(9)
O(5)#1−Zn(1)−O(6)	86.17(7)	N(1)−Cu(1)−N(4)	93.51(9)
O(5)−Zn(1)−O(6)	73.20(7)	N(3)−Cu(1)−N(4)	84.82(9)
N(5)#1−Zn(1)−O(6)#1	92.30(9)		

[a] Symmetry transformations used to generate equivalent atoms: #1 $-x+1, y, -z+1/2$.

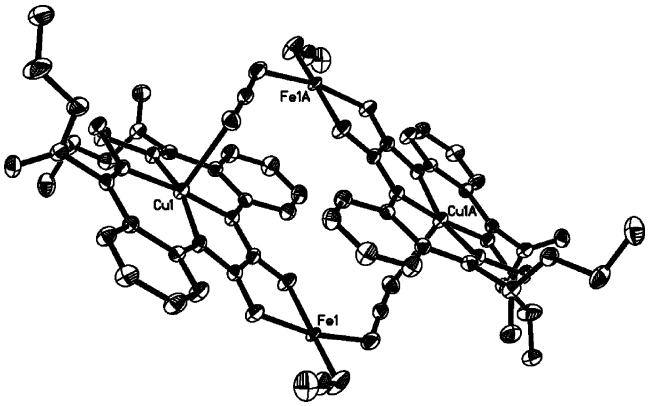

Figure 6. Tetranuclear molecule of **4**.

Table 5. Selected Bond Lengths (Å) and Angles (deg) for **4**[a]

Cu(1)−N(2)	1.946(3)	Fe(1)−N(5)	1.929(4)
Cu(1)−N(4)	1.952(3)	Fe(1)−N(8)	1.941(4)
Cu(1)−N(3)	1.960(3)	Fe(1)−O(6)	1.975(3)
Cu(1)−N(1)	1.966(3)	Fe(1)−O(5)	1.980(3)
Cu(1)−N(10)#1	2.394(4)		
N(2)−Cu(1)−N(4)	173.10(14)	N(3)−Cu(1)−N(10)#1	92.58(14)
N(2)−Cu(1)−N(3)	85.65(14)	N(1)−Cu(1)−N(10)#1	102.97(14)
N(4)−Cu(1)−N(3)	92.38(14)	N(5)−Fe(1)−N(8)	93.71(19)
N(2)−Cu(1)−N(1)	92.97(14)	N(5)−Fe(1)−O(6)	92.80(16)
N(4)−Cu(1)−N(1)	87.16(13)	N(8)−Fe(1)−O(6)	169.15(14)
N(3)−Cu(1)−N(1)	164.43(14)	N(5)−Fe(1)−O(5)	172.19(17)
N(2)−Cu(1)−N(10)#1	91.75(14)	N(8)−Fe(1)−O(5)	91.76(15)
N(4)−Cu(1)−N(10)#1	94.95(14)	O(6)−Fe(1)−O(5)	80.97(12)

[a] Symmetry transformations used to generate equivalent atoms: #1 $-x, -y+2, -z+1$.

are given in Table 5. The oxamido and $\mu_{1,3}$-N^{3-} alternate bridged Cu(II) and Fe(II) units, which results in the formation of a cyclic tetranuclear molecule. The Fe(II) atom coordinates with two oxygen donors of the macrocyclic oxamide ligand and two nitrogen atoms from two N^{3-} ions. Furthermore, one of the coordinated N^{3-} ions acts as terminal ligand, and the other one $\mu_{1,3}$-bridges the Fe(II) and Cu(II) atoms. The distance between the Fe(II) and Cu(II) atoms bridged by N^{3-} is 5.205 Å, while that of those bridged by oxamido is 5.236 Å. The Cu(II) atom resides in a slightly distorted square pyramidal environment. Four nitrogen donors from the macrocyclic ligand coordinate to the Cu(II) atom as the square base of the pyramid. One nitrogen donor from the N^{3-} coordinates to the Cu(II) atom as the apex of the pyramid. The deviations of Fe1 and Cu1 from the least-squares plane defined by C1, C2, O5, O6, N1, and N4 are −0.2631 and 0.0539 Å, respectively. As shown in Figure 7, the adjacent tetranuclear molecules form a 1D chain through the weak coordinated bond between Fe(II) atom and the oxygen atom from the ester carbonyl of the macrocyclic ligands.

To our knowledge, **1**, **2**, and **3** are the first structurally characterized macrocyclic oxamido-bridged trinuclear [M^{II}-Cu^{II}_2] complexes. Simultaneously, the oxamido and dca bridges in **2** both connect the heterometallic atoms to form a 2D layer structure, while oxamido and azide bridges in **4** result in 1D chain strcture. The assembly of these modes, in which two different bridge ligands both connect the heterometallic atoms, is also rarely reported.

Magnetic Properties of 1. The temperature dependence of the molar magnetic susceptibility (χ_M) and the effective magnetic moment (μ_{eff}) for **1** and **2** are shown in Figure 8. The μ_{eff} value of **1** at room temperature is 6.04 μ_B, lower than the spin-only value (6.40 μ_B) expected for the uncoupled $Cu^{II}Mn^{II}Cu^{II}$ trinuclear system ($S_{Cu} = 1/2$ and $S_{Mn} = 5/2$). The μ_{eff} value decreases smoothly upon cooling and reaches a near plateau value of 3.84 μ_B below 16 K. The plateau moment is close to the spin-only value for $S_T = 3/2$ (3.87 μ_B) resulting from the antiferromagnetic spin coupling between Cu(II) and Mn(II) ions in the trinuclear system. Below 6 K, the effective magnetic moment decreases markedly, which may be the result of the intermolecular interactions between the trinuclear molecules.

On the basis of the crystal structure of **1** (Figure 2), there are two kinds of magnetic interactions for the present system from a magnetic viewpoint, namely, (i) the intramolecular Cu(II)−Mn(II)−Cu(II) interactions through oxamido bridges and (ii) the intermolecular interactions between the adjacent trinuclear molecules through the $\pi-\pi$ interactions. Taking into account the two kinds of interactions, we try to analyze the experimental cryomagnetic data using the isolated heterobinuclear complex with only Cu(II)−Mn(II)−Cu(II) through two oxamido bridges. The magnetic analysis was then carried out by using the theoretical expression of the magnetic susceptibility deduced from the spin Hamiltonian $\hat{H} = -2J\hat{S}_{Mn}(\hat{S}_{Cu(1)} + \hat{S}_{Cu(2)} + \beta[g_{Cu}(\hat{S}_{Cu(1)} + \hat{S}_{Cu(2)}) + g_{Mn}\hat{S}_{Cu}]\cdot \boldsymbol{H}$. The expression of the magnetic susceptibility was obtained as follows: [1a,27]

$$\chi_{tri} = [N\beta^2/(4KT)][A/B] + N_\alpha \qquad (N_\alpha = 120 \times 10^{-6})$$

$$A = 10(g_{3/2,1})^2_2 + 35(g_{5/2,1})^2 \exp[5J/(KT)] + 35(g_{5/2,0})^2 \exp[7J/(2KT)] + 84(g_{7/2,1})^2 \exp[12J/(KT)]$$

$$B = 2 + 3\exp[5J/(KT)] + 3\exp[7J/(KT)] + 4\exp[12J/(KT)]$$

$g_{ss'}$ are molecular g factors ($S' = S_{Cu1} + S_{Cu2}$, $S = S' + S_{Mn}$), $g_{ss'} = C_a g_{mn} + C_b$, and g_{Cu}, g_{Mn}, and g_{Cu} are the local g factors

(27) Sinn, E.; Harris, C. M. *Coord. Chem. Rev.* **1969**, *4*, 391.
(28) O'Connor, C. J. *Prog. Inorg. Chem.* **1982**, *29*, 203.

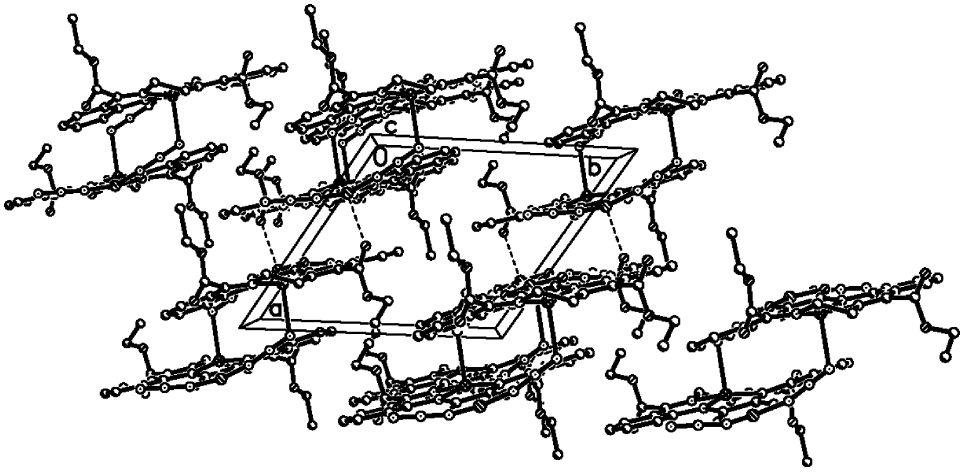

Figure 7. Perspective view of the molecule packing of **4** along the *c* axis.

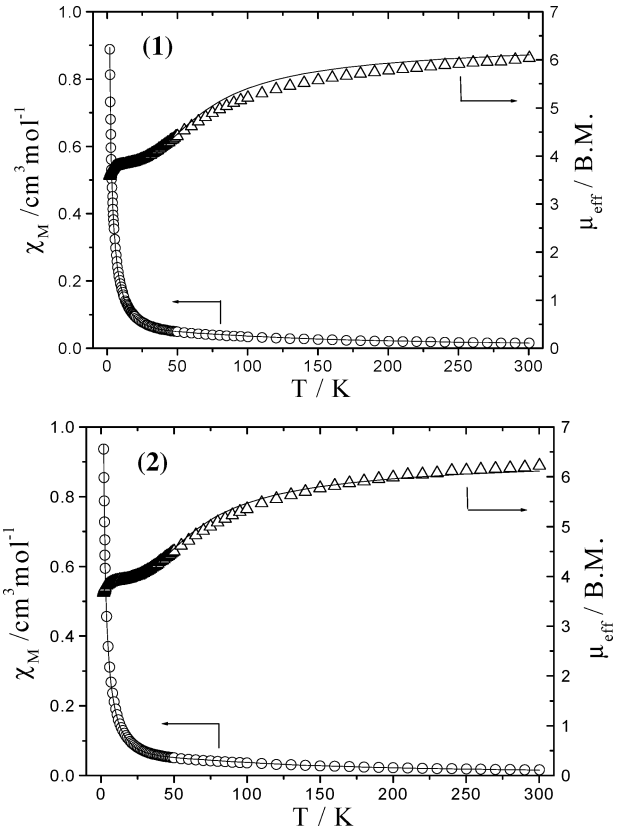

Figure 8. χ_M (○) vs T and μ_{eff} (Δ) vs T plots for **1** and **2**.

assumed to be isotropic. The C_a and C_b coefficients are readily calculated as follows[29]

$$g_{3/2,1} = (7g_{Mn} - 2g_{Cu})/5$$
$$g_{5/2,1} = (31g_{Mn} + 4g_{Cu})/35$$
$$g_{7/2,1} = (5g_{Mn} + 2g_{Cu})/7$$
$$g_{5/2,0} = g_{Mn} \quad (1)$$

where N is Avogadro's number, β the Bohr magneton, k the Boltzmann constant, J the exchange integral between Mn(II) and Cu(II) ions, T the absolute temperature, N_α (120×10^{-6})[30] the temperature-independent paramagnetism, and g_{Mn} and g_{Cu} are the local g factors assumed to be isotropic. Second, because of the very weak magnetic interactions between the adjacent trinuclear molecules, the expression (eq 1) must be corrected for the magnetic exchange. The molecular field approximation may be used for this purpose and is illustrated in eq 2.[28]

$$\chi = \chi_{tri}/[1 - (2zJ')/(Ng^2\beta^2)\,\chi_{tri}] \quad (2)$$

where χ is the exchange-coupled magnetic susceptibility actually measured, χ_{tri} is also the magnetic susceptibility in the absence of the molecular field, zJ' is the exchange parameter between trinuclear molecular unit, and the rest of the parameters have their usual meanings. Here, the g factor is supposed to be 2. Magnetic data were well fitted to eq 2 in the temperature range of 2−300 K with the best parameters $J = -23.8$ cm^{-1}, $g_{Mn} = 2.00$, $g_{Cu} = 2.06$, and $zJ' = -0.07$ cm^{-1}. Agreement factor, defined as $R = \Sigma(\chi_{obsd} - \chi_{calcd})^2/\Sigma\chi_{obsd}^2$, is 1.75×10^{-4}. The J value suggests a pronounced intramolecular antiferromagnetic interaction between the copper(II) and manganese(II) ions through the oxamido bridges, and the zJ' value suggests a very weak intermolecular antiferromagnetic interaction through the $\pi-\pi$ interactions.

Magnetic Properties of 2. The μ_{eff} value at room temperature is 6.23 μ_B, lower than the spin-only value (6.40 μ_B) expected for the uncoupled $Cu^{II}Mn^{II}Cu^{II}$ trinuclear unit ($S_{Cu} = 1/2$ and $S_{Mn} = 5/2$). The μ_{eff} value decreases smoothly upon cooling and reaches a near plateau value of 3.94 μ_B below 16 K. The plateau moment is close to the spin-only value for $S_T = 3/2$ (3.87 μ_B) resulting from the antiferromagnetic spin coupling in the trinuclear system. Below 6 K, the effective magnetic moment decreases markedly.

On the basis of the crystal structure of **2** (Figure 4), there should be four kinds of magnetic interactions for the present system, namely, (i) Mn1···Cu1 through the oxamido bridge in one trinuclear unit, (ii) Mn1···Cu2 through the oxamido

(29) Bencini, A.; Gatteschi, D. *EPR of Exchange Coupled Systems*; Springer-Verlag: Berlin, 1990.

(30) (a) Sinn, E.; Harris, C. M. *Coord. Chem. Rev.* **1969**, *4*, 391. (b) Matsumoto, N.; Inoue, K.; Ohba, M.; Okawa, H.; Kida, S. *Bull. Chem. Soc. Jpn.* **1992**, *65*, 2283.

Table 6. Structural and Magnetic Information for Some Oxamido-Bridged Species[a]

	oxamide	structure	structure unit	*J* between Mn^{II} and Cu^{II} (cm^{-1})	ref
$[Mn(Me_6\text{-}[14]ane\text{-}N_4)Cu(oxpn)]\ (CF_3SO_3)_2$	noncyclic	binuclear	[MnCu]	−31/2	6h
$MnCu(obbz)(H_2O)_3\cdot DMF$	noncyclic	1D	[MnCu]	−32/2	6f
$[Mn\{Cu(HL^3)(DMF)\}_2(DMF)_2]$	noncyclic	trinuclear	$[MnCu_2]$	−14	8d
$\{[Cu(oxbe)]Mn(H_2O)[Cu(oxbe)\ (DMF)]\}_n\cdot nDMF\cdot nH_2O$	noncyclic	2D	$[MnCu_2]$	−17.4	8e
$[(CuL^1)Mn(bpy)_2](ClO_4)_2$	cyclic	binuclear	[MnCu]	−13.9	13b
$[(CuL^1)Mn(phen)_2](ClO_4)_2\cdot 1.5H_2O$	cyclic	binuclear	[MnCu]	−14.2	13a
$[(CuL^1)Mn(ntb)](ClO_4)_2\cdot H_2O$	cyclic	binuclear	[MnCu]	−14.7	13a
$[(CuL^2)Mn(N_3)_2]_n$	cyclic	1D	[MnCu]	−25.6	20
$[Mn(CuL^1)_3]\ (N_3)_2\cdot EtOH$	cyclic	tetranuclear	$[MnCu_3]$	−16.3	15
$[Mn(CuL^2)_3](ClO_4)_2$	cyclic	tetranuclear	$[MnCu_3]$	−14	16
$Mn(CuL)_2(SCN)_2$	cyclic	trinuclear	$[MnCu_2]$	−23.8	this work
$\{[Mn(CuL)_2(\mu\text{-dca})_2]2H_2O\}_n$	cyclic	2D	$[MnCu_2]$	−22.5	this work

[a] The structures of L, L^1, and L^2 are shown in Scheme 1. H_4L^3 is *N*,*N*′-bis[2-(hydroxyiminomethyl)phenyl] oxamide.

bridge in one trinuclear unit, (iii) Mn1···Cu1 through the dca bridges between the adjacent trinuclear units, and (iv) Mn1···Cu2 through the dca bridges between the adjacent trinuclear units. To the best of our knowledge, there is no formula in the literature to deal with the magnetic susceptibility of such a complicated system, so we used an approximate method.

We take the heterotrinuclear $[Mn^{II}Cu^{II}_2(\mu\text{-oxamidato})_2]$ unit as a whole, there are two kinds of magnetic interactions in this system, which is carried out by the method used in **1**. The best fit for the experimental data gives $J = -22.5\ cm^{-1}$, $g_{Mn} = 2.00$, $g_{Cu} = 2.03$, and $zJ' = -0.04\ cm^{-1}$. The agreement factor, defined as $R = \sum(\chi_{obsd} - \chi_{calcd})^2/\sum\chi_{obsd}^2$, is 3.09×10^{-4}. The *J* value suggests a pronounced antiferromagnetic interaction between copper(II) and manganese(II) ions through the oxamido bridges, and the zJ' value suggests a very weak antiferromagnetic interaction through the $\mu_{1,5}$-dca bridges.

For complex **1**, the distances of Cu···Cu and Cu···Mn between the adjacent molecules are 3.943 and 5.720 Å, respectively, while for complex **2** the distances of Cu···Cu and Cu···Mn between the adjacent trinuclear molecules are 7.561 and 7.906 Å, respectively, which are much larger than those in **1**. Furthermore, the bridging ligand dca is not an effective media to transfer magnetic interactions. So the bridged complex **2** has weaker intermolecular magnetic interaction than the isolated complex **1**.

The oxamido group has been noted to be an efficient mediator of magnetic exchange between paramagnetic centers.[1a] It is also well-known that the molecular topology has an important influence on the magnetic properties. Some manganese(II)−copper(II) species incorporating noncyclic oxamide or macrocyclic oxamide ligands reported previously are listed in the Table 6. The exchange integral in **1** and **2** is in the range of those reported previously. According to Kahn, the antiferromagnetic interaction between Cu(II) and Mn(II) arises from the nonzero overlap between the magnetic orbitals centered at the two metal ions and delocalized toward the ligands. A larger overlap of the magnetic orbitals leads to stronger interaction. In a comparison with the $[Mn(Me_6\text{-}[14]\ ane\text{-}N_4)Cu(oxpn)](CF_3SO_3)_2$ *J* value of $-31.1/2\ cm^{-1}$ reported by Kahn and his colleagues, the absolute values of the exchange integral of **1** and **2** are higher.

Acknowledgment. This work was supported by the National Natural Science Foundation of China (Nos. 20471031, 20331010, and 20631030).

Supporting Information Available: Crystallographic files in CIF format. This material is available free of charge via the Internet at http://pubs.acs.org.

IC061792M